

# Phase Relationships in the $\text{ZrO}_2$ -Rich Part of the Systems Y–Zr–N–O, Ca–Zr–N–O, and Mg–Zr–N–O up to Temperatures of 1150°C

J. Wrba and M. Lerch\*

Silicatchemie, Universität Würzburg, Germany

(Received 24 December 1997; accepted 20 March 1998)

## Abstract

*Nitridation of yttria, calcia, and magnesia stabilised zirconia takes place at temperatures above 1400°C in nitrogen atmosphere. Depending on the composition, the formed quaternary compounds possess crystal structures with ordered ( $\beta$ -type phases) or randomly distributed (tetragonal and cubic phases) anion vacancies derived from the fluorite-type structure of cubic  $\text{ZrO}_2$ . Incorporation of nitrogen or magnesia into  $\text{ZrO}_2$  leads to a decrease of the cell volume, whereas an incorporation of yttria or calcia causes an increase of the unit cell dimensions. Phase relationships and thermal expansion coefficients of quaternary compounds in the systems Y–Zr–N–O, Ca–Zr–N–O, and Mg–Zr–N–O are presented up to temperatures of 1150°C. The incorporation of yttria shows the strongest effect on the stabilisation of the high temperature phases and decreases considerably the transition temperature to these phases. In the systems Ca–Zr–N–O and Mg–Zr–N–O, these effects are less pronounced. © 1998 Elsevier Science Limited. All rights reserved*

## 1 Introduction

Yttria, calcia, and magnesia stabilised zirconia ceramics are commonly used in engineering because of their outstanding electrical and mechanical properties.<sup>1</sup> Due to charge neutrality reasons, doping  $\text{ZrO}_2$  with aliovalent cations leads to the formation of anion vacancies. Furthermore, incorporation of nitrogen is another way to form anion vacancies. Direct nitridation of zirconia in nitrogen atmosphere at temperatures above 1400°C leads to  $\text{ZrN}_{2n/3}\text{O}_{2-n}$  phases ( $\text{ZrO}_2$ – $\text{Zr}_3\text{N}_4$  system) with trigonally distorted fluorite-type structures

and ordered anion vacancies ( $\beta$ -type phases).<sup>2–7</sup> Depending on the type of vacancy ordering, the  $\text{ZrN}_{2n/3}\text{O}_{2-n}$  phases are called  $\beta''$ ,  $\beta'$ , or  $\beta$  phase. The nitridation of yttria stabilised zirconia, which led to compounds with the general composition  $\text{Y}_m\text{Zr}_{1-m}\text{N}_{2n/3}\text{O}_{2-(m/2)-n}$ , was carried out first by Cheng and Thompson.<sup>2–4</sup> With increasing synthesis temperature, the nitrogen content increases. At the same time, the yttria content necessary to stabilise the tetragonal or cubic high temperature phase at room temperature decreases. The effects of cation- and anion-related vacancies on the stabilisation are additive. If the yttria content amounts to 1 mol% and lower, trigonally distorted fluorite-type structures with ordered anion vacancies ( $\beta$ -type phases) exist. The synthesis of oxynitrides in the systems Ca–Zr–N–O and Mg–Zr–N–O and their characterisation at room temperature were recently reported by Lerch *et al.*<sup>8</sup> In this case, compounds with general compositions of  $\text{Ca}_m\text{Zr}_{1-m}\text{N}_{2n/3}\text{O}_{2-m-n}$  and  $\text{Mg}_m\text{Zr}_{1-m}\text{N}_{2n/3}\text{O}_{2-m-n}$  were produced. For these quaternary systems, another paper<sup>9</sup> explains the vacancy ordering as a function of chemical parameters, discussing the different structure-types known from the  $\text{ZrO}_2$ – $\text{Zr}_3\text{N}_4$  system and the pure oxide systems. In the calcia containing system,  $\beta''$ ,  $\beta'$ , and  $\beta$  phases with ordered anion vacancies and cubic samples with randomly distributed vacancies were observed. In the Y–Zr–N–O system,  $\beta''$ ,  $\beta'$ , tetragonal, and cubic phases exist. Only  $\beta''$  and  $\beta'$  phases were found in the magnesia containing system. The formed structure-type is determined by the quotient of the vacancy concentration, caused by the incorporation of nitrogen, and the total vacancy concentration. In contrast, the transition tetragonal+cubic $\leftrightarrow$ cubic depends on an effective total vacancy concentration, respecting also the individual effects of the different dopant ions.<sup>9</sup>

\*To whom correspondence should be addressed.

In this work, the behaviour of vacancy ordering and the stability range of the different phases at temperatures up to 1150°C are presented for the systems Y–Zr–N–O, Ca–Zr–N–O, and Mg–Zr–N–O. Most work was done in the yttria-containing system. In contrast to Mg/Ca-samples, these quaternary materials show interesting electrical properties.<sup>10</sup>

## 2 Experimental

Zirconia powder (Alfa, 99.9%) was mixed with Y<sub>2</sub>O<sub>3</sub> (H. C. Starck, 99.9%), CaO (Merck, 99.8%), and MgO (Alfa, 99.9%) in 2-propanol, dried, and pressed isostatically into pellets. The pellets, containing 0–15 mol% of the respective dopant oxides were sintered in air at 1750°C for 3 days. After grinding and isostatical pressing, these pellets were nitrided in nitrogen atmosphere in a graphite heated resistance furnace (KCE) at temperatures between 1600 and 1900°C, and nitrogen pressures between 1.2 and 4.5 bar. The sintering time amounted to 1–4 h, the cooling time about 3 h. Phase analysis and high temperature investigations were carried out in an X-ray powder diffractometer (STOE Stadi P) with Cu-K<sub>α1</sub> radiation. During the high temperature measurements, the samples were located in closed capillaries under nitrogen atmosphere. The phase contents were determined by the polymorph method described by Garvie and Nicholson.<sup>11</sup> In this calculation, the β-type phases were treated as cubic zirconia. The nitrogen content was determined by hot gas extraction (LECO). This method is described elsewhere.<sup>8</sup>

## 3 Results and Discussion

### 3.1 Synthesis and characterisation

After nitridation of the ZrO<sub>2</sub>–Y<sub>2</sub>O<sub>3</sub> solid solutions, the samples consist of the phases described above. Figure 1 shows the amount of baddeleyite-type phase as a function of the yttria content for different synthesis conditions. As shown by Scott<sup>12</sup> for the Y–Zr–O system, the region of completely stabilised zirconia is reached with 7.5 mol% yttria. After sintering in nitrogen atmosphere, only 3 mol% yttria are needed to obtain fully stabilised zirconia. Analogous to the systems Ca–Zr–N–O and Mg–Zr–N–O,<sup>8</sup> the content of monoclinic ZrO<sub>2</sub> decreases with increasing synthesis temperature, nitridation time, and nitrogen pressure. As described by Cheng and Thompson,<sup>4</sup> the nitrogen content increases with increasing nitriding temperature. For identical conditions of synthesis, the nitrogen concentration of the quaternary samples decreases with increasing yttria content. Illustrating this

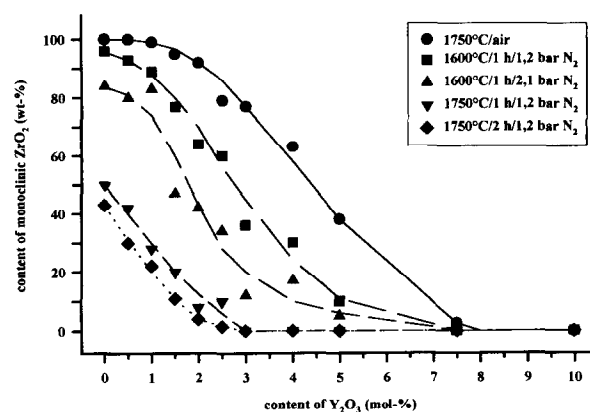


Fig. 1. Content of monoclinic ZrO<sub>2</sub> as a function of the Y<sub>2</sub>O<sub>3</sub> concentration for different synthesis conditions.

behaviour, Fig. 2 presents the concentration of the anion vacancies caused by incorporation of nitrogen [ $V_N$ ] as a function of the vacancy concentration caused by the incorporation of yttria [ $V_Y$ ] at 1900°C. The calculated data result from the thermodynamic description given by Lerch *et al.*<sup>8</sup> There is an acceptable agreement between experimental and calculated data. Assuming a nearly ideal behaviour of the defects at 1900°C, the coefficient  $K$  for the nitridation of yttria doped zirconia can be determined. At 1900°C, 4 bar nitrogen pressure, and  $5 \times 10^{-15}$  bar oxygen pressure,  $K$  amounts to  $1 \times 10^{-25}$ . In the systems Ca–Zr–N–O and Mg–Zr–N–O, the coefficients are in the same order of magnitude.<sup>8</sup>

In all the investigated systems, high nitridation temperatures (>1900°C) and nitrogen pressures (>4 bar) lead to the formation of rocksalt-type Zr<sub>2</sub>Y(N<sub>2</sub>O<sub>2</sub>C) phases with varying compositions (Lerch and Wrba).<sup>13</sup> Therefore, it is difficult to produce single-phase quaternary compounds with high nitrogen concentrations and low dopant oxide

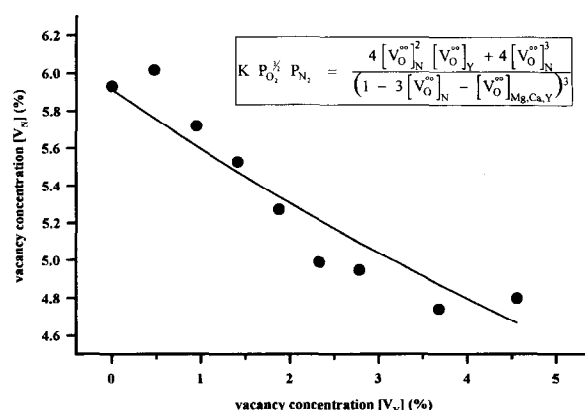


Fig. 2. Concentration of anion vacancies caused by nitrogen [ $V_N$ ] as a function of the vacancy concentration caused by Y<sub>2</sub>O<sub>3</sub> [ $V_Y$ ] at a temperature of 1900°C (experimental and calculated data, [ $V_N$ ] = 100 [ $V_O^\infty$ ]<sub>N</sub>, [ $V_Y$ ] = 100 [ $V_O^\infty$ ]<sub>Y</sub>, details are given in Lerch *et al.*).<sup>8</sup>

contents. Cheng and Thompson<sup>4</sup> suspected that the fluorite structure tolerates only a total vacancy concentration of 6% in the anion lattice. Above this limit, ZrN or related phases precipitate. In our investigations, samples with a total anion vacancy concentrations of 10% and more were observed without precipitation of ZrN. The limit is higher than assumed. On the other hand, ZrN derived phases also exist in samples with concentrations lower than 6%.

The lattice constants of the monoclinic baddeleyite phase are not influenced by the nitridation. However, the lattice constants of the nitrogen containing compounds depend on the ionic radii of the dopant ions and also on the concentration of anion vacancies. In general, in a lattice derived from the fluorite-type structure, anion vacancies lead to a decrease of the lattice constants. For cubic phases with 10 mol%  $\text{Y}_2\text{O}_3$ , Fig. 3 shows the decrease of the unit cell dimensions with increasing nitrogen content. Because of the similarity between the ionic radii of  $\text{O}^{2-}$  (138 pm, coordination number CN=IV) and  $\text{N}^{3-}$  (146 pm (CN=IV)),<sup>14</sup> the effect of increasing vacancy concentration on the cell constants dominates. The same behaviour is observed in the Ca–Zr–N–O system.<sup>8</sup> In contrast, with increasing concentration of  $\text{Y}^{3+}$  or  $\text{Ca}^{2+}$  ions, the lattice constants increase. As an example, Fig. 4 depicts the lattice parameters of some  $\beta''$ -phases with increasing yttria content. The effect of the dopant ions dominates because of the larger ionic radii of  $\text{Y}^{3+}$  and  $\text{Ca}^{2+}$  [102 pm and 112 pm (CN=VIII), respectively] compared with the ionic radius of  $\text{Zr}^{4+}$  [84 pm (CN=VIII)]. All other observed phases in the yttria and calcia containing systems ( $\beta'$ ,  $\beta$ , tetragonal, cubic) show a similar behaviour. In contrast, the lattice parameters decline with increasing magnesia content in the Mg–Zr–N–O system. For example, Fig. 5 shows the cell constants of quaternary compounds with  $\beta'$

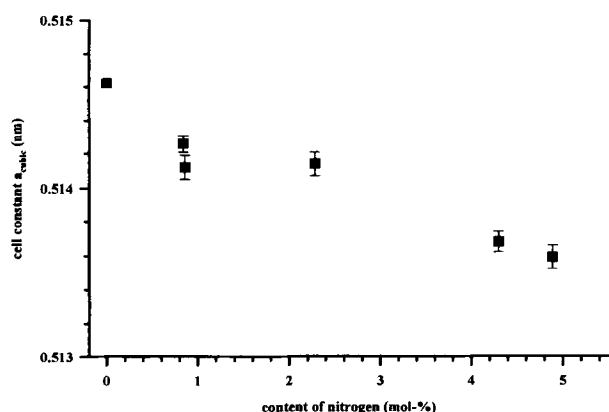


Fig. 3. Variation of the cell constant of cubic Y–Zr–N–O phases for different amounts of nitrogen. The content of  $\text{Y}_2\text{O}_3$  amounts to 10 mol%.

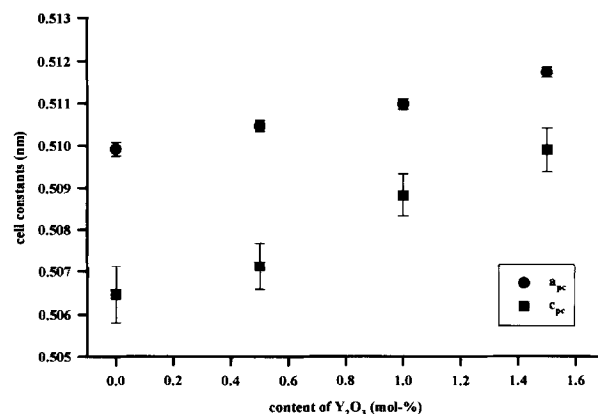


Fig. 4. Variation of the cell constants of trigonal Y–Zr–N–O phases ( $\beta''$  structure) for different amounts of yttria. The trigonal constants are plotted in a pseudo-cubic fluorite-type setting ( $a_{\text{pc}} = a_{\text{trig}}/\sqrt{7/2}$ ,  $c_{\text{pc}} = c_{\text{trig}}/5\sqrt{3}$ ).

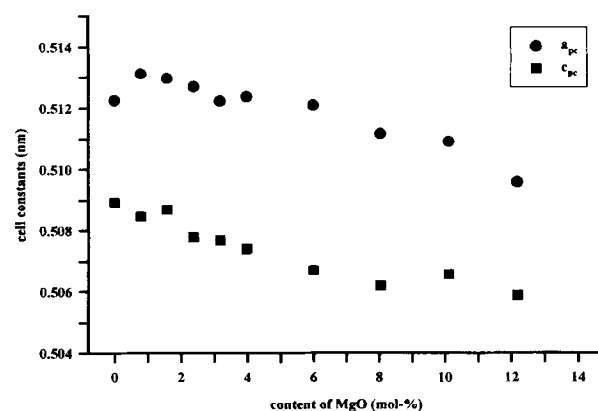


Fig. 5. Lattice constants of trigonal Mg–Zr–N–O phases ( $\beta'$  structure) as a function of the magnesia concentration. The trigonal constants are plotted in a pseudo-cubic fluorite-type setting ( $a_{\text{pc}} = a_{\text{trig}}/\sqrt{7/2}$ ,  $c_{\text{pc}} = c_{\text{trig}}/2\sqrt{3}$ ).

structure. In this case, the effect of increasing vacancy concentration dominates the effect of cation doping because of the similar ionic radii of  $\text{Mg}^{2+}$  and  $\text{Zr}^{4+}$  [89 and 84 pm (CN=VIII), respectively].<sup>14</sup>

### 3.2 High temperature investigations

Figures 6–9 present the phase relationships in the observed systems as a function of temperature in a nitrogen atmosphere. It should be remarked that no equilibrium phase diagrams can be presented because of the very low diffusion coefficients of the cations in fluorite-type structures. For instance, the synthesis of  $\text{Y}_4\text{Zr}_3\text{O}_{12}$  with an ordered cation distribution needs several months at 1000°C.<sup>15</sup> It is assumed that equilibrium could not be reached during the considerably shorter high temperature experiments (~14 h per sample). Furthermore, it is difficult to determine the exact stability fields of tetragonal and cubic phases. Because of severe peak overlap in the X-ray diagrams, small contents of cubic phase can hardly be detected beside large contents of tetragonal phase and vice versa. The

quasi binary sectional plane  $\text{ZrO}_2\text{--Zr}_3\text{N}_4$  in Fig. 6 corresponds well with the results of Lerch and Rahäuser.<sup>6</sup> However, the boundaries monoclinic ( $m$ ) + tetragonal ( $t$ )  $\leftrightarrow$  tetragonal and tetragonal  $\leftrightarrow$  tetragonal + cubic ( $c$ ) are shifted to lower temperatures with increasing nitrogen content and reach the range of transition between phases with ordered anion vacancies and phases with randomly distributed vacancies. Independent of the nitrogen concentration, this range exists at about 1000°C.

Alloying with yttria, a decrease in the order/disorder (O/D) transition temperature ( $\beta$ -type phases  $\leftrightarrow$  tetragonal, cubic) with increasing yttria concentration is observed [Fig. 7(a)–(c)]. Above a content of 3 mol%  $\text{Y}_2\text{O}_3$ , this transition takes place below room temperature. In contrast to the yttria-free  $\text{Zr--N--O}$  system, another boundary exists in the low temperature region between phases with ordered vacancies and phases with randomly distributed vacancies at discrete nitrogen concentrations. Phases without vacancy ordering are observed for low nitrogen concentrations. An increase of the yttria content leads to a shift of the boundary to higher nitrogen contents. This behaviour reflects again the fact that this boundary is determined by the ratio of the different dopant concentrations.<sup>9</sup> However, with increasing yttria content, the intersections of the oxide system with the phase transformation  $m + t \leftrightarrow t$  and  $t \leftrightarrow t + c$  shift to lower temperatures. The stability range of the tetragonal phase becomes smaller and disappears above 3 mol%  $\text{Y}_2\text{O}_3$ . The fact that Fig. 7(b and c) are not consistent with equilibrium phase diagram principles could be explained by the larger amount of  $\text{Y}_2\text{O}_3$  in comparison to Fig. 7(a). The time to reach equilibrium prolongs with increasing yttria content. For example, we are not able to understand the existence of the  $m + t$  region at higher nitrogen content than the tetragonal phase field in Fig. 7(b and c). Nevertheless, the positions of the phase boundaries correspond well with the

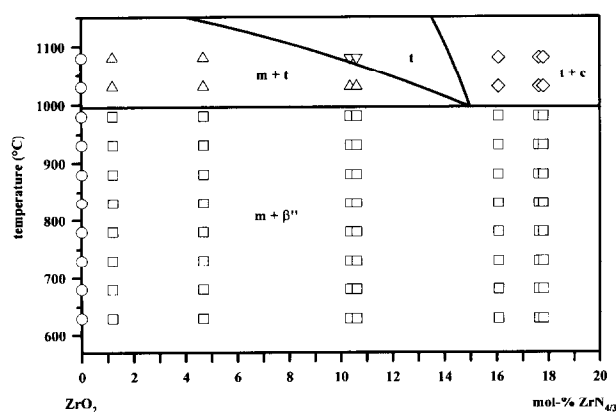


Fig. 6. Phase relationships in the  $\text{ZrO}_2$ -rich part of the quasi binary  $\text{ZrO}_2\text{--Zr}_3\text{N}_4$  system ( $\circ$  = baddeleyite phase,  $m$  = monoclinic,  $t$  = tetragonal,  $c$  = cubic).

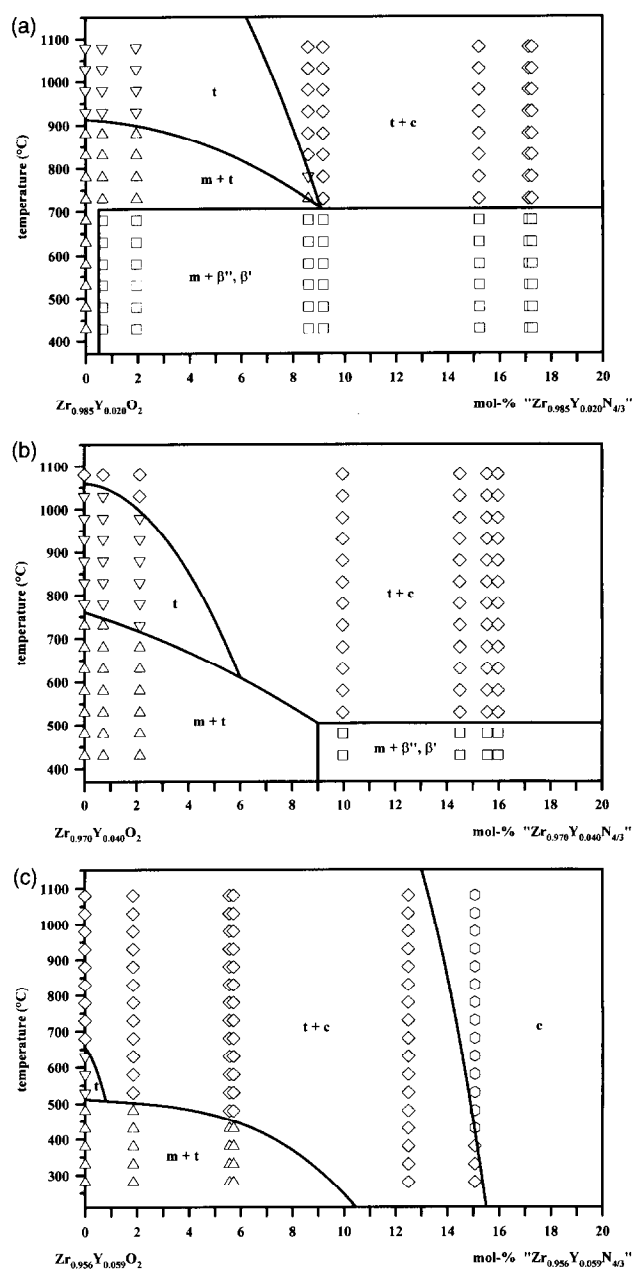


Fig. 7. Phase relationships in the  $\text{ZrO}_2$ -rich part of quasi binary sectional planes in the  $\text{Y--Zr--N--O}$  system with constant  $\text{Y}_2\text{O}_3$  contents: (a) 1 mol%  $\text{Y}_2\text{O}_3$ , (b) 2 mol%  $\text{Y}_2\text{O}_3$  and (c) 3 mol%  $\text{Y}_2\text{O}_3$  ( $m$  = monoclinic,  $t$  = tetragonal,  $c$  = cubic).

results of samples with 1.5 and 2.5 mol%  $\text{Y}_2\text{O}_3$ , which are not shown here. Similar investigations are carried out for the systems  $\text{Ca--Zr--N--O}$  and  $\text{Mg--Zr--N--O}$ . The results are shown in Figs 8 and 9. Because of the smaller number of samples, only parts of the systems can be presented.

In the  $\text{Ca--Zr--N--O}$  system, the transformation temperature  $m + t \leftrightarrow t$  decreases with increasing calcia content to the range of the O/D transition. The temperature of the O/D transition slightly decreases with increasing calcia content. In Fig. 8, the tetragonal regions cannot be better positioned without more experimental results. However, the transformations  $m + t \leftrightarrow t$  and  $t \leftrightarrow t + c$  shift to

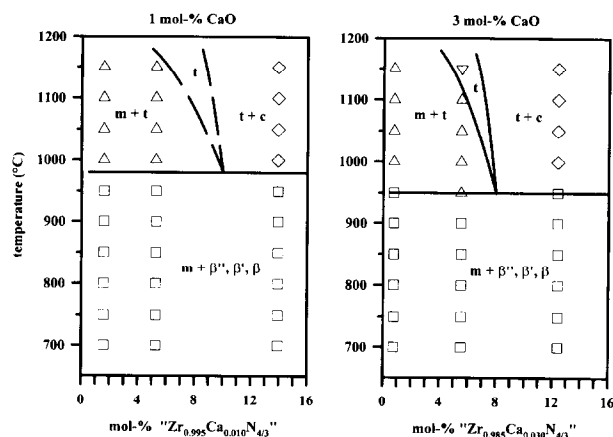


Fig. 8. Phase relationships in the  $\text{ZrO}_2$ -rich part of quasi binary sectional planes in the Ca-Zr-N-O system with constant CaO contents: 1 mol% CaO (left) and 3 mol% CaO (right) ( $m$  = monoclinic,  $t$  = tetragonal,  $c$  = cubic).

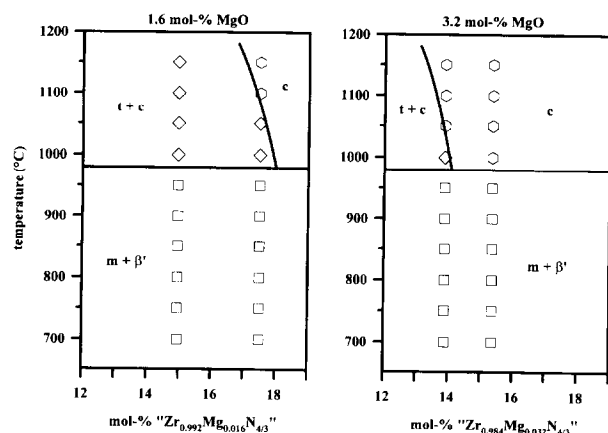


Fig. 9. Phase relationships in the  $\text{ZrO}_2$ -rich part of quasi binary sectional planes in the Mg-Zr-N-O system with constant MgO contents: 1.6 mol% MgO (left) and 3.2 mol% MgO (right) ( $m$  = monoclinic,  $t$  = tetragonal,  $c$  = cubic).

lower nitrogen concentrations with increasing calcia content.

In the Mg-Zr-N-O system, the content of magnesia has only a small effect on the O/D transition at 950–1000°C. With increasing magnesia content, the transformation  $t + c \leftrightarrow c$  shifts to lower nitrogen contents. Corresponding to the  $\text{ZrO}_2$ - $\text{Zr}_3\text{N}_4$  system, the transformation temperature decreases with increasing nitrogen concentration. Details of the behaviour of the  $\beta$ -type phases in the individual systems are given in.<sup>9</sup>

The transition tetragonal-cubic is mainly determined by the concentration of anion vacancies and also influenced by the size, charge and concentration of the dopant ions (Kountouros and Petzow).<sup>16</sup> As described in the introduction, incorporation of nitrogen, yttria, calcia, or magnesia leads to the formation of anion vacancies. Looking at the  $t + c \leftrightarrow c$  transition in the three investigated systems, the behaviour, even at high temperatures, agrees well with the concept of the effective

vacancy concentration, which is described by Lerch *et al.*<sup>9</sup> for ambient temperature. This empirical concept also respects the individual effects of the dopant ions. As depicted in Fig. 10, only one discrete value of the effective vacancy concentration exists at c.g. 1080°C, determining the transition into the cubic phase field. In contrast, the total vacancy concentration shows a broad range for the transition  $t + c \leftrightarrow c$ . The high temperature investigations in a temperature range between 25°C and 1080°C show that this concept is valid in the whole temperature range, whereas the effective concentration decreases slightly with increasing temperature (25°C:  $V_{\text{total-eff.}} = 1.1$ ;<sup>8</sup> 1080°C:  $V_{\text{total-eff.}} = 0.96$ ). In the Ca-Zr-N-O and Mg-Zr-N-O system, the effective vacancy concentration is nearly identical with the total vacancy concentration.<sup>9</sup>

It is known from intensively studied ternary zirconia systems that vacancy ordering is accompanied by an additional ordering process in the anion or cation sublattice. This is shown for the Ca-Zr-O system by Marxreiter *et al.*,<sup>17</sup> for the Y-Zr-O system by Scott,<sup>18</sup> and for nitrogen containing zirconia by Lerch *et al.*<sup>19</sup> Consequently, the mobility of cations and anions plays an important role for the ordering kinetics in these materials. In anion-deficient fluorite-type structures, the anion mobility is more than six orders of magnitude larger compared with the cation mobility (1000°C).<sup>20</sup> Hence, ternary zirconium oxynitrides show fast ordering kinetics, whereas pure oxide materials need long annealing times for the ordering of anion vacancies on a long range order scale. The behaviour of the quaternary oxynitride phases mainly depends on the individual dopant concentrations in the cation and anion sublattice, respectively.

Determination of lattice constants during the heating experiments is important for a better understanding of the individual phase transitions. For the transition  $t \rightarrow c$ , the cell constants of the

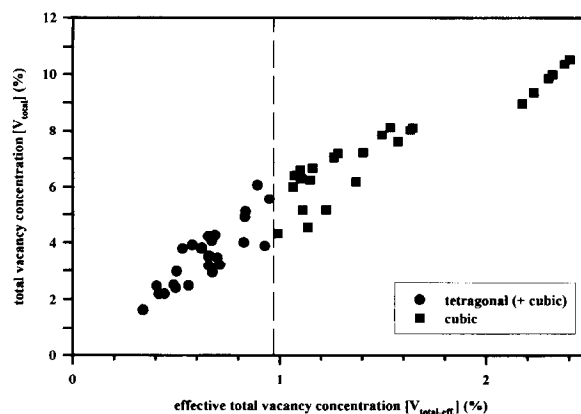


Fig. 10. Tetragonal and cubic phases in the system Y-Zr-N-O as a function of the total vacancy concentration  $[V_{\text{total}}]$  and the effective total vacancy concentration  $[V_{\text{total-eff.}}]$  at 1080°C.

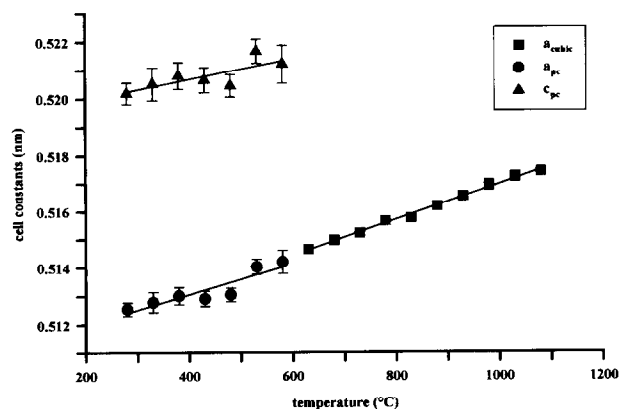


Fig. 11. Variation of the cell constants of a tetragonal Y-Zr-N-O phase during heating (contents: 2.5 mol%  $\text{Y}_2\text{O}_3$ , 6.1 mol% N). The tetragonal constants are plotted in a pseudo-cubic fluorite-type setting ( $a_{\text{pc}} = a_{\text{tetra}}\sqrt{2}$ ,  $c_{\text{pc}} = c_{\text{tetra}}$ ).

involved phases are shown in Fig. 11 as a function of temperature. The sample contains 2.5 mol%  $\text{Y}_2\text{O}_3$  and 6.1 mol% nitrogen; tetragonal lattice constants are plotted in a pseudo-fluorite setting. The phase transition is connected with a volume shrinkage of about 1% in which the tetragonal constant  $a_{\text{pc}}$  turns into the cubic cell constant  $a_{\text{cubic}}$ . The transition  $t \rightarrow c$  in the pure oxide Y-Zr-O system is displacive and without diffusion (Heuer *et al.*<sup>21</sup>). Hence, a similar behaviour is suggested for the Y-Zr-N-O system.

At ambient temperature, most samples in the three investigated systems consist of a mixture of a baddeleyite-type phase and a phase with ordered anion vacancies ( $\beta''$ ,  $\beta'$ , or  $\beta$ ). Heating these mixtures above 600°C, the cell volume of the baddeleyite phases in the nitrogen containing system is slightly smaller than the volume in the pure oxide system. Above 600°C, a small but significant solubility of nitrogen in the monoclinic phase seems to exist, which is not strongly influenced by the content of dopant cations. The transition temperature to the high temperature phases with randomly distributed vacancies depends on the composition of the samples, mostly pronounced in the Y-Zr-N-O system. For comparison, the results for the ternary Zr-N-O system are given by Walter *et al.*<sup>22</sup> For the Y-Zr-N-O system, Figs 12 and 13 show the transition from  $\beta''$  phase to tetragonal and cubic phases, respectively. In the tetragonal case, the sample contains 0.5 mol%  $\text{Y}_2\text{O}_3$  and 4.3 mol% nitrogen, in the cubic case 1 mol%  $\text{Y}_2\text{O}_3$  and 7.9 mol% nitrogen. The phase transitions are connected with a volume increase of about 1.5 ( $\beta'' \rightarrow$  tetragonal) and 3% ( $\beta'' \rightarrow$  cubic). Similar processes take place during the transitions of all  $\beta''$ ,  $\beta'$ , and  $\beta$  phases in the systems Y-Zr-N-O, Ca-Zr-N-O and Mg-Zr-N-O. These transitions are connected with diffusion of oxygen and nitrogen.

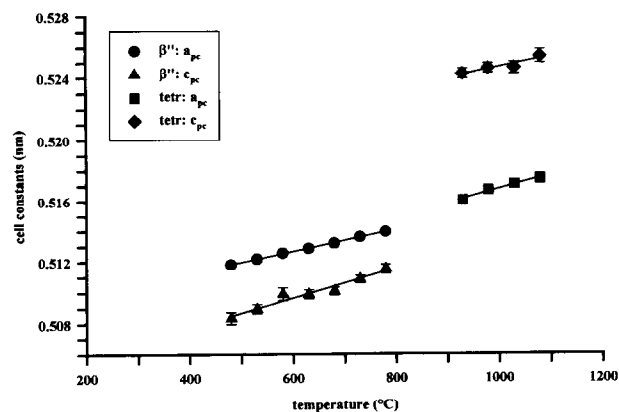


Fig. 12. Variation of the cell constants of a trigonal Y-Zr-N-O phase ( $\beta''$  structure) during heating (contents: 0.5 mol%  $\text{Y}_2\text{O}_3$ , 4.3 mol% N). The cell constants are plotted in a pseudo-cubic fluorite-type setting ( $\beta''$ :  $a_{\text{pc}} = a_{\text{trig}}/\sqrt{7/2}$ ,  $c_{\text{pc}} = c_{\text{trig}}/5\sqrt{3}$ ; tetragonal:  $a_{\text{pc}} = a_{\text{tetra}}\sqrt{2}$ ,  $c_{\text{pc}} = c_{\text{tetra}}$ ).

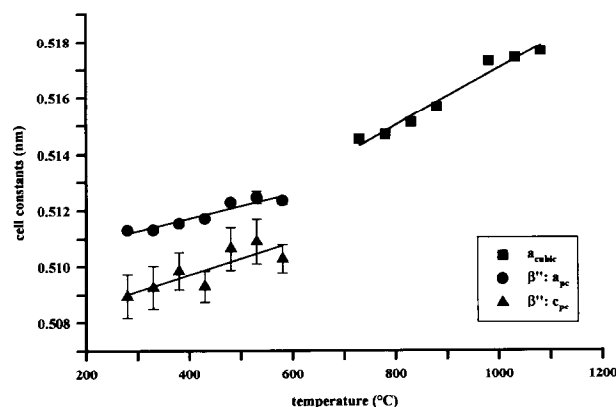


Fig. 13. Variation of the cell constants of a trigonal Y-Zr-N-O phase ( $\beta''$  structure) during heating (contents: 1 mol%  $\text{Y}_2\text{O}_3$ , 7.9 mol% N). The trigonal constants are plotted in a pseudo-cubic fluorite-type setting ( $\beta''$ :  $a_{\text{pc}} = a_{\text{trig}}/\sqrt{7/2}$ ,  $c_{\text{pc}} = c_{\text{trig}}/5\sqrt{3}$ ).

Finally, the thermal expansion of tetragonal and cubic samples was investigated. According to Garvie,<sup>23</sup> the thermal expansion increases with increasing vacancy concentration. As an example, Fig. 14 shows the volume expansion coefficients as a function of vacancy concentration for tetragonal and cubic phases in the yttria containing system. In all investigated quaternary systems, this behaviour is also valid for phases with ordered vacancies. In the system Y-Zr-N-O for instance, the volume expansion coefficients of  $\beta'$  and  $\beta''$  phases amount to  $\sim 40 \times 10^{-6} \text{ K}^{-1}$  and  $\sim 46 \times 10^{-6} \text{ K}^{-1}$ , respectively. Comparing the volume expansion coefficient of the  $\beta'$  phase in the individual systems, thermal expansion is the largest in the yttria containing system and less pronounced in the magnesia containing system with  $\sim 24 \times 10^{-6} \text{ K}^{-1}$ . The coefficient in the calcia containing system amounts to  $\sim 33 \times 10^{-6} \text{ K}^{-1}$ . This behaviour can be also observed for high temperature phases in the pure oxide systems (Garvie).<sup>23</sup>

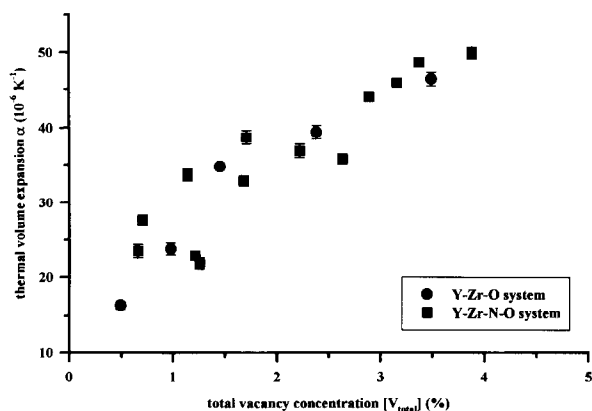


Fig. 14. Thermal volume expansion coefficients of tetragonal and cubic phases in yttria containing systems as a function of the total vacancy concentration  $[V_{\text{total}}]$  (temperature range: 680–1080°C).

### Acknowledgements

The authors thank Mrs J. Lerch for experimental help. Thanks are also due to Professor G. Müller and the Deutsche Forschungsgemeinschaft (DFG) for financial support.

### References

1. Stevens, R., *Introduction to Zirconia*. Magnesium Elektron Publication No. 113, Manchester, 1986.
2. Cheng, Y. and Thompson, D. P., Nitrogen-containing tetragonal zirconia. *Journal of Am. Ceram. Soc.*, 1991, **74**, 1135–1138.
3. Cheng, Y. and Thompson, D. P., The nitriding of zirconia. *Special Ceramics*, 1992, **9**, 149–162.
4. Cheng, Y. and Thompson, D. P., Role of anion vacancies in nitrogen-stabilised zirconia. *Journal of Am. Ceram. Soc.*, 1993, **76**, 683–688.
5. Lerch, M., Nitridation of zirconia. *Journal of Am. Ceram. Soc.*, 1996, **79**, 2641–2644.
6. Lerch, M. and Rahäuser, O., Subsolidus phase relationships in the  $\text{ZrO}_2$  rich part of the system  $\text{ZrO}_2\text{--Zr}_3\text{N}_4$ . *Journal of Mater. Sci.*, 1997, **32**, 1357–1363.
7. Lerch, M., Krumeich, F. and Hock, R., Diffusion controlled formation of  $\beta$  type phases in the system  $\text{ZrO}_2\text{--Zr}_3\text{N}_4$ . *Solid State Ionics*, 1997, **95**, 87–93.
8. Lerch, M., Lerch, J., Hock, R. and Wrba, J., Synthesis and characterisation of oxynitrides in the  $\text{ZrO}_2$  rich part of the systems Ca–Zr–O–N and Mg–Zr–O–N. *Journal of Solid State Chem.*, 1997, **128**, 282–288.
9. Lerch, M., Wrba, J. and Lerch, J., Vacancy ordering in the  $\text{ZrO}_2$  rich part of the systems Ca–Zr–O–N, Mg–Zr–O–N, and Y–Zr–O–N. *Journal of Solid State Chem.*, 1996, **125**, 153–158.
10. Wendel, J., Lerch, M. and Laqua, W., Novel zirconia based superionic conductors: the electrical conductivity of Y–Zr–N–O materials, submitted to *Journal of Solid State Chem.*
11. Garvie, R. C. and Nicholson, P. S., Phase analysis in zirconia systems. *Journal of Am. Ceram. Soc.*, 1972, **55**, 303–305.
12. Scott, H. G., Phase relationships in the zirconia–yttria system. *Journal of Mater. Sci.*, 1975, **10**, 1527–1535.
13. Lerch, M. and Wrba, J., Formation of rock salt-type  $\text{Zr}(\text{N},\text{O},\text{C})$  phases by carbothermal nitridation of zirconia. *Journal of Mater. Sci. Lett.*, 1996, **15**, 378–380.
14. Shannon, R. D., Revised effective ionic radii and systematic studies of interatomic distances in halides and chalcogenides. *Acta Cryst.*, 1976, **A32**, 751–767.
15. Stubican, V. S., Phase equilibria and metastabilities in the systems  $\text{ZrO}_2\text{--MgO}$ ,  $\text{ZrO}_2\text{--CaO}$ , and  $\text{ZrO}_2\text{--Y}_2\text{O}_3$ . In *Advances in Ceramics 24B, Science and Technology of Zirconia III*, ed. S. Somiya, N. Yamamoto and H. Yanagida. The Am. Ceram. Soc., Columbus, 1988, pp. 71–82.
16. Kountouros, P. and Petzow, G., Defect chemistry, phase stability and properties of zirconia polycrystal. In *Science and Technology of Zirconia V*, ed. S. P. S. Badwal, M. J. Bannister and R. H. J. Hannink. Technomic Publishing, 1993, pp. 30–48.
17. Marxreiter, H., Boysen, H., Frey, F. and Vogt, T., The structure of the  $\Phi_1$ -phase  $\text{CaZr}_4\text{O}_9$  in calcium stabilized zirconia. *Mat. Res. Bull.*, 1990, **25**, 435–442.
18. Scott, H. G., The yttria–zirconia  $\delta$  phase. *Acta Cryst.*, 1977, **B33**, 281–282.
19. Lerch, M., Boysen, H. and Radaelli, P., High temperature neutron scattering investigation of the  $\beta'$  phase in the Mg–Zr–N–O system. *Journal of Phys. Chem. Solids*, in press.
20. Oishi, Y., Ando, K. and Sakka, Y., Lattice and grain boundary diffusion coefficients of cation stabilized zirconias. In *Advances in Ceramics 12*, ed. N. Claussen, M. Rühle & A. H. Heuer. The Am. Ceram. Soc., Columbus, 1983, pp. 208–219.
21. Heuer, A. H., Chaim, R. and Lanteri, V., Review: phase transformations and microstructural characterisation of alloys in the system  $\text{Y}_2\text{O}_3\text{--ZrO}_2$ . In *Advances in Ceramics 24B, Science and Technology of Zirconia III*, ed. S. Somiya, N. Yamamoto and H. Yanagida. The Am. Ceram. Soc., Columbus, 1988, pp. 3–20.
22. Walter, D., Lerch, M. and Laqua, W., Thermal stability of the  $\beta''$  phase in the  $\text{ZrO}_2\text{--Zr}_3\text{N}_4$  system. *Journal of Thermal Anal.*, 1997, **48**, 709–716.
23. Garvie, R. C., Zirconium dioxide and some of its binary systems. In *High Temperature Oxides Part II*, ed. A. M. Alper, Academic Press, New York, 1970, pp. 117–166.